Published in final edited form as:
Chem Phys Lett. 2012 February 27; 527: 22–26. doi:10.1016/j.cplett.2011.12.061.

Solvation Structure and Energetics of Single Ions at the Aqueous Liquid-Vapor Interface

Brad A. Bauer, **Shuching Ou**, and **Sandeep Patel***
Department of Chemistry and Biochemistry, University of Delaware, Newark, Delaware 19716, USA

Abstract

Potentials of mean force for single, *nonpolarizable* monovalent halide anions and alkali cations are computed for transversing the water-air interface (modeling using polarizable TIP4P-FQ and TIP4P-QDP). Iodide and bromide in TIP4P-FQ show interfacial stability, whereas chloride, bromide, and iodide show interfacial stability in TIP4P-QDP. A monotonic decrease in coordination number and an increasingly anisotropic distribution of solvating water molecules is shown to accompany movement of the ions towards vapor conditions; these effects are most noticeable with increases in ion size/decreases in magnitude of hydration free energy.

Keywords

Ions; Polarizable Force Fields; Molecular Dynamics; TIP4P-FQ; TIP4P-QDP; Potential of Mean Force; Solvation Structure

I. INTRODUCTION

Liquid-vapor (LV) interfacial regions of aqueous salt solutions have been widely studied due to their applicability in environmental, biological, and industrial processes.[1–3] An emerging consensus based on spectroscopic measurements,[4–6] molecular simulations,[7–11] and theoretical studies[12,13] suggests that the density of large, charge-diffuse anions (such as bromide or iodide) is enhanced at the interface, whereas that of small, charge-dense ions (such as fluoride and alkali-series cations) is reduced in the interfacial region. Molecular dynamics (MD) simulations have been widely employed for such studies since they offer an approach to directly probe the depth-dependent ion density and solvation properties with atomistic resolution. For instance, Dang demonstrated the stability of iodide and bromide and a repulsion of chloride at the LV interface via potential of mean force (PMF) calculations of single ions using polarizable water-ion models;[7] however, the stability of iodide dissipated when an additive pair potential was implemented. Using polarizable TIP4P-FQ water, Warren and Patel observed increased enhancement of chloride and iodide density in the LV interface when these ions were treated as polarizable.[14] Vrbka et al. also

*Corresponding author. sapatel@udel.edu.

V. SUPPORTING INFORMATION AVAILABLE Additional anisotropy profiles and RADFs for ions studied at sampled windows for TIP4P-FQ and TIP4P-QDP systems.

demonstrate differences using various permutations for treating ion and solvent polarizability.[8] In general, simulation studies using polarizable potentials support interfacial presence of anions (chloride, bromide, iodide).[7,9,10,14] This is not a requirement, however, as interfacial enhancement of ions has been observed using fixed-charge (non-polarizable) models.[11,15] Using non-polarizable ions developed for use in the SPC/E water model, whose solvation free energetics were thoroughly characterized,[16] Horinek and Netz observed an interfacial minimum of 0.48 kcal/mole (2 kJ/mole) in the PMF for iodide.[11] More indirectly, several studies have demonstrated enhanced presence of iodide anion near hydrophobic surfaces and interfaces, which are considered as sufficiently "liquid-vapor like" environments[17]. In particular, the nature of the first solvation shell of ions (both in bulk and interface) has been implicated in the propensity of ions for the LV interface. Wick and Xantheas suggest that the inherent anisotropic solvation of large polarizable ions such as iodide can influence their propensity for the LV interface.[18]. We have previously studied inorganic ions at the water liquid-vapor interface using polarizable water and non-polarizable ion force fields[14,19,20]. We employ polarizable water force fields based on the charge equilibration (fluctuating charge) formalism. The first water model is that of Rick et al[21] and the second is a water model that allows variation of intrinsic molecular polarizability (excluding intermolecular charge transfer) with local electrochemical environment, the TIP4P-QDP water model[22]. We find that with water-ion interaction models that have been carefully constructed to reproduce gas-phase water-ion dimer energies and structures as well as condensed phase hydration free energetics (with the caveats associated with para-meterization of ion force fields using single ion absolute hydration free energies as reference data), one can observe significant interfacial ion density enhancement when only water polarizability is explicitly included in the force field. Our experience has shown that ion polarizability is not necessarily the sole driving force for interfacial specific ion effects. However, observed behaviors of anions at the water liquid-vapor interface arise from a complex interplay between water and ion properties (and force fields).

In the spirit of studying interfacial behavior of aqueous salt solutions, we characterize properties of single ions at the LV interface for ions force fields used in conjunction with the TIP4P-FQ force field.[14,19,23,24] We examine single ion potentials of mean force through the water liquid-vapor interface as well as metrics of solvation structure (water coordination, radial angular distributions, and hydration anisotropy) along this path. Additionally, we draw a qualitative comparison of the PMF and solvation properties of the TIP4P-FQ-ion systems with those of TIP4P-QDP.[20] These systems show differences in anionic enhancement at the liquid-vapor interface for 1M salt solutions, and such a comparison lends insight into the relationship between ion hydration and interfacial activity.

II. RESULTS

A. Single Ion Properties at the TIP4P-FQ Aqueous Liquid-Vapor Interface

The potential of mean force (PMF) was calculated for each ion as a function of its z-position using the weighted histogram analysis method (WHAM);[25] results are shown in Figure 1. Iodide shows a pronounced minimum at z=23.4Å, which occurs about 2Å below the position of the Gibbs Dividing Surface (GDS). This minimum is approximately 0.5 kcal/mol more favorable than bulk, and approximately 0.74 kcal/mol more favorable than experienced at z = 17Å, where the PMF experiences a local maximum. The position of the minimum relative to the GDS is in good agreement with the position of a peak in iodide density observed by Warren and Patel for 1M NaI solutions at the liquid-vapor interface (using the same force field).[19] Furthermore, the position of the maximum in the iodide PMF corresponds to the position of a minimum in the 1M density profiles. The next largest anion, bromide, shows a broad well with a minimum at $z \approx 23$Å; this minimum is approximately 0.25 kcal/mol. The

two smaller anions, fluoride and chloride, show no pronounced minimum. Dang also observed minima for single bromide and iodide PMFs across the LV interface using polarizable water and ion, with no minimum observed for chloride; the magnitudes of the minima were greater relative to those seen here (−0.9 and −1.5 kcal/mol versus −0.2 and −0.5 kcal/mol for bromide and iodide, respectively). Interestingly, Horinek et al predict a significant minimum of about 0.5 kcal/mol for iodide at the LV interface using non-polarizable ions in SPC/E water; cations and smaller halides experienced repulsion across the LV interface.[11] We note that each anion experiences a significant barrier as it moves across the the liquid-vapor interface. The onset of these barriers occurs earliest for fluoride, and increases with increasing ion size. This order is anticipated on the basis of hydration free energies. Of the anions, fluoride, which has the most favorable hydration free energy, experiences the greatest desolvation penalty. Similar behavior is observed for the cations, which all experience a monotonic increase in PMF as they move across the LV-interface.

In order to assess the change in hydration of ions as they move across the LV-interface, we calculate the z-position dependent average number of water molecules within the first coordination shell of the ion (Figure 2). For this analysis, we define the first solvation shell cutoff distance as the position of the first minimum in the radial distribution function for single ions in TIP4P-FQ.[24] In bulk solution, we calculate coordination numbers in good agreement with those from previous studies (see Table I).[24] Moving throught the GDS into the vapor, the coordination number decreases. All ions remain partially hydrated in the vapor; anions maintain about four coordinating water molecules, whereas cations maintain approximately five coordinating water molecules. Larger ions, inherently having more water molecules in the first solvation shell, show greatest changes in the coordination number upon transfer into the vapor phase. We posit that this is a consequence of the weaker attraction of water to the larger ions (evidenced by the hydration free energies). Completely desolvated ions are not observed in our simulations. This is in agreement with calculations for transferring hydrated ion clusters from bulk water to 1,2-dichloroethane,[26] and simulations of ions across water/air interface.[7]

In order to investigate the solvation structure of ions as they move across the LV interface, radial angular distribution functions (RADF) of water molecules around an ion were calculated for each ion at various z-positions. Here, r is the distance between a given ion and a water oxygen, and θ denotes the angle formed between the ion-oxygen vector and the positive z-axis. This property is plotted in Figure 3 for fluoride and iodide in (z = 10 Å), in the LV interface (z = 25 Å), and in the vapor phase (z = 35 Å); additional profiles for other ions are included in the Supporting Information. We notice qualitatively similar behavior as the anions traverse the LV interface. In the bulk, water isotropically hydrates the ions. The intensity of the inner rings map to the magnitude of the first peak in a radial distribution function; the rarefied regions between the first and second rings corresponds to the first minima in the RDFs. In this context, the RADFs agree with the RDFs of Warren and Patel.[24] In particular, fluoride shows intense solvation within the first hydration shell and pronounced first minimum. With increasing anion size, the intensity of the first hydration ring decreases and the rarefied region becomes less pronounced. As ions enter the LV interfacial region, their solvation structure becomes disrupted. The second solvation shell becomes depleted in the positive z-direction (corresponding to the upper portion of the RADF profiles and the direction of the vapor phase). Similar partial dehydration occurs in the first solvation shell; the probability of water hydrating the ion in the direction of the vapor phase is reduced. This loss in hydration is compensated with a more favorable binding of water molecules to the ion in the bulk direction. Iodide shows the most significant disruption to the first solvation shell on the vapor side, suggesting the relatively weak binding of water molecules to this ion. As the ion moves into the vapor region the probability of finding water in the positive z-direction increases (relative to that in the LV

interface). Furthermore, the water molecules coordinating the ion are strongly bound to it, particularly in the negative z-direction; this attracts additional water molecules from the bulk into the second solvation shell. Similar results are seen for the cations. The smallest cation studied, sodium, shows the strongest hydration within the first shell. Cesium demonstrates solvation behavior similar to bromide/iodide, although depletion of cesium's first hydration shell (in the z direction at the LV interface) is not as severe. This can be anticipated from the similar size and hydration free energies of these ions.

To further characterize the solvation of these ions, we examine the anisotropy of the solvating water molecules. We adopt the approach of Beck et al.,[27–29] which we briefly summarize here. All water molecules are rotated into a local coordinate frame by setting the vector of ion to the closest water's center of mass (COM) as the x-axis. Using the vector from the ion to the second closest water's COM, the second water is constrained to lie in the $x-y$ plane with positive y. The projection of third water's COM is then made a positive value by reflection about the z-axis. The projection of all COMs along the < 1, 1, 1 > direction is determined, resulting in one-dimensional plots of the projected distance of water cluster COM from the ion as a function of the number of closest water molecules comprising that cluster. The projected values are positive when water molecules tend to accumulate in the direction of the three closest water molecules and negative for the opposite direction. Values of zero indicate that the center of mass of the n hydrating water molecules coincides with the position of the ion; that is, there is isotropic distribution of water molecules around the ion. Results for the solvation of ions in each environment are shown in Figure 4. For the anions in the bulk (panel a), these profiles reach a minimum when the ion's first solvation shell is filled; a second minimum is reached when the ion's second solvation shell is satisfied. Ions show near-isotropic solvation beyond the filling of the second solvation shell. In the LV interface, the depletion of water above the ion leads to increased anisotropy in the first solvation shells; the magnitude of this anisotropy increases with increasing ionic size, in agreement with our observations from RADFs. Since water solvates the ion in only the negative z and $x-y$ directions, the center of mass of the water cluster moves further from the ion as more water molecules are considered. In the vapor phase, the anisotropy is further increased for large n. Also, the minimum occurs at $n \approx 4$ for all the anions, which corresponds to the average coordination number at that position. In analogous environments, the cations are generally more isotropically solvated than the anions. Cesium deviates most significantly from the other cations in terms of anisotropic solvation in the first coordination shell and at large n. The large size and weak hydration free energy of this ion allows it to be more easily dehydrated (as observed in the RADFs).

B. Single Ion Properties at the TIP4P-QDP Aqueous Liquid-Vapor Interface

As a final analysis, we compare TIP4P-FQ and TIP4P-QDP water-ion results. Results from 1M solutions NaX (X={Cl^-,Br^-,I^-}) salts in TIP4P-QDP water showed a significant enhancement of anion density in the interfacial region,[20] whereas analogous enhancement in simulations of salts in TIP4P-FQ showed only enhancement for iodide (chloride showed no enhancement).[14] These differences in interfacial ion enhancement are reflected in the PMFs for single ions at the LV interface (Figure 1a). In particular, all anions show a pronounced (> kT) minimum approaching the LV interface. Furthermore, the anions in TIP4P-QDP are able to further penetrate the vapor region than the anions in TIP4P-FQ. We note that calculated hydration free energies for a given anion are less favorable for the TIP4P-QDP set than TIP4P-FQ. We further compare the coordination of ions as they move across the LV interface in Figure 2a. Normal to its coordination number in bulk, a given anion's coordination decreases more rapidly for the TIP4P-QDP than TIP4P-FQ. We note that the global minimum in the PMF profiles of the TIP4P-QDP systems occurs at positions in which the average coordination number of the ion is reduced relative to the bulk. Comparing

the anisotropy of ion hydration (up to the first shell) in the liquid vapor interface, we observe similar behavior for chloride in both TIP4P-FQ and TIP4P-QDP solvents. This suggests that solvation structure alone cannot account for differences in chloride enhancement at the LV interface for these models. Despite the similarities in chloride solvation for the two models, water molecules hydrating bromide and iodide in TIP4P-QDP in the LV interface are more anisotropic than those in TIP4P-FQ. This correlates with a greater depletion of water in the first solvation shell for the TIP4P-QDP systems as evidenced by the radial angular distribution functions.

III. DISCUSSION AND CONCLUSIONS

In conclusion, we have studied properties of single ions at the liquid-vapor interface using non-polarizable ions in conjunction with the TIP4P-FQ model. This combination of ion and water force field has previously been characterized on the basis of single ion hydration free energies[24] and structural and electrostatic properties for 1M salt solutions.[14,19] In agreement with density profiles of 1M salt solutions at the interface[14], we observe an interfacial minimum in the PMF for iodide, whereas chloride favors the bulk. In the interfacial region, the solvation of anions is disrupted and anisotropic. Larger anions demonstrate a greater degree of partial hydration in the direction of the vapor phase than smaller anions. Furthermore, the average number of water molecules coordinating an ion decreases monotonically as it moves through the LV interface. Each ion retains several coordinating water molecules in the vapor phase (approximately four for anions and approximately five for cations). These properties were also computed for ions in TIP4P-QDP water.[20] Unlike the TIP4P-FQ/ion sets, all anions in TIP4P-QDP show a pronounced minimum approximately 2 Å below the GDS. These ions have less favorable hydration free energies than analogous ions in TIP4P-FQ and also demonstrate a sharper decrease in coordination number as they move across the LV interface.

VI. METHODS

Molecular dynamics simulations were performed using the CHARMM package.[30] Simulations of liquid-vapor interfaces were performed in the NVT ensemble. Temperature was maintained at T = 298K using a Nosé-Hoover thermostat.[31] The simulation cell was rectangular with dimensions 24 Å × 24 Å × 100 Å, in which z is the direction normal to the liquid-vapor interface. A bulk slab consisting of 988 water molecules (represented by the polarizable TIP4P-FQ model[21]) and a single ion (Na^+, K^+, Cs^+, F^-, Cl^-, Br^-, I^-) was positioned in the center of the simulation cell, resulting in two liquid-vapor interfaces. Ions were treated as non-polarizable particles with interaction parameters based on those by Lamoureux and Roux[23] and validated for use with TIP4P-FQ by Warren and Patel.[14,19,24] Lennard-Jones interactions were gradually switched off over the range 10 Å to 11Å. In all simulations, ions were constrained to z-positions from 10Å-35Å relative to the system center of mass using a harmonic potential with force constants ranging from 1-5 (kcal/mol)/$Å^2$; this encompasses a range approximately 15 Å below the Gibbs Dividing Surface to approximately 10 Å above it. Potential of mean forces were calculated using the Weighted Histogram Analysis Method (WHAM).[25] Charge degrees of freedom for the TIP4P-FQ water molecules were coupled to a thermostat at 1K with mass 0.005 kcal/mol/ps^2 using the Nosé-Hoover method. Conditionally convergent long-range electrostatic interactions were treated using Particle Mesh Ewald (PME)[32] approach with a 30 × 30 × 128 point grid, 6th order interpolation, and κ = 0.33. Dynamics were propagated using a Verlet leap-frog integrator with a 0.5 fs timestep. Total sampling time for each window was 3-12 ns; properties were calculated from all but the first nanosecond, which was treated as equilibration. Parameters for simulations of ions in TIP4P-QDP were taken from Bauer and Patel.[20] A harmonic restoring potential was implemented to prevent unfavorable

overpolarization of the TIP4P-QDP water. This potential with force constant 200.0 (kcal/mol)/esu^2 was turned on beyond upper and lower charge limits $-0.6e$ and $-1.6e$ for the *M*-site and $1.2e$ and $0.3e$ for hydrogen sites. All other simulation details were consistent with those previously described for ions in TIP4P-FQ.

Supplementary Material

Refer to Web version on PubMed Central for supplementary material.

Acknowledgments

The authors acknowledge support from the National Institutes of Health (COBRE:5P20RR017716-07) at the University of Delaware, Department of Chemistry and Biochemistry. B.A.B. acknowledges additional support from a Graduate Fellows Award at the University of Delaware.

References

[1]. Finlayson-Pitts BJ. The chemistry of sea salt: A molecular-level view of the chemistry of NaCl and NaBr. Chem. Rev. 2003; 103:4801–4822. [PubMed: 14664634]

[2]. Jungwirth P, Tobias DJ. Specific ion effects at the air/water interface. Chem. Rev. 2006; 106:1259–1281. [PubMed: 16608180]

[3]. Chang T, Dang LX. Recent advances in molecular simulations of ion solvation at liquid interfaces. Chem. Rev. 2006; 106:1305. [PubMed: 16608182]

[4]. Petersen PB, Saykally RJ. Confirmation of enhanced anion concentration at the liquid water surface. Chem. Phys. Lett. 2004; 397:51–55.

[5]. Petersen PB, Saykally RJ. On the nature of ions at the liquid water surface. Annu. Rev. Phys. Chem. 2006; 57:333–364. [PubMed: 16599814]

[6]. Ghosal S, Hemminger JC, Bluhm H, Mun BS, Hebenstreit ELD, Ketteler G, Ogletree DF, Requejo FG, Salmeron M. Electron spectroscopy of aqueous solution interfaces reveals surface enhancement of halides. Science. 2005; 307:563–566. [PubMed: 15681380]

[7]. Dang LX. Computational study of ion binding to the liquid interface of water. J. Phys. Chem. B. 2002; 106:10388–10394.

[8]. Vrbka L, Mucha M, Minofar B, Jungwirth P, Brown EC, Tobias DJ. Propensity of soft ions for the air/water interface. Curr. Opin. Colloid Inter. Sci. 2004; 9:67–73.

[9]. Jungwirth P, Tobias DJ. Ions at the air/water interface. J. Phys. Chem. B. 2002; 106:6361–6373.

[10]. Jungwirth P, Tobias DJ. Molecular structure of salt solutions: A new view of the interface with implications for heterogeneous atmospheric chemistry. J. Phys. Chem. B. 2001; 105:10468–10472.

[11]. Horinek D, Herz A, Vrbka L, Sedlmeier F, Mamatkulov SI, Netz RR. Specific ion adsorption at the air/water interface: The role of hydrophobic solvation. Chem. Phys. Lett. 2009; 479:173–183.

[12]. Levin Y, dos Santos AP, Diehl A. Ions at the air-water interface: an end to a hundred-year-old mystery? Phys. Rev. Lett. 2009; 103:257802. [PubMed: 20366288]

[13]. Levin Y. Polarizable ions at interfaces. Phys. Rev. Lett. 2009; 102:147803. [PubMed: 19392484]

[14]. Warren GL, Patel S. Comparison of the solvation structure of polarizable and nonpolarizable ions in bulk water and near the aqueous liquid-vapor interface. J. Phys. Chem. C. 2008; 112:7455–7467.

[15]. Eggimann BL, Siepmann JI. Size effects on the solvation of anions at the aqueous liquid-vapor interface. J. Phys. Chem. C. 2008; 112:210–218.

[16]. Horinek D, Mamatkulov SI, Netz RR. Rational design of force fields based on thermodynamic solvation properties. J. Chem. Phys. 2009; 130:124507. [PubMed: 19334851]

[17]. Huang DM, Cottin-Bizonne C, Ybert C, Bocquet L. Aqueous electrolytes near hydrophobic surfaces: dynamic effects of ion specificity and hydrodynamic slip. Langmuir. 2008; 24:1442–1450. [PubMed: 18052395]

[18]. Wick CD, Xantheas SS. Computational investigation of interfacial and bulk chloride and iodide first solvation shell aqueous structure. J. Phys. Chem. B. 2009; 113:4141–4146. [PubMed: 19014185]

[19]. Warren GL, Patel S. Electrostatic properties of aqueous salt solution interfaces: A comparsion of polarizable and nonpolarizable ion models. J. Phys. Chem. B. 2008; 112:11679–11693. [PubMed: 18712908]

[20]. Bauer BA, Patel S. Molecular dynamics simulations of nonpolarizable salt solution interfaces: NaCl, NaBr, and NaI in transferable intermolecular potential 4-point with charge dependent polarizability TIP4P-QDP water. J. Chem. Phys. 2010; 132:8107–8117.

[21]. Rick SW, Stuart SJ, Berne BJ. Dynamical fluctuating charge force fields: Application to liquid water. J. Chem. Phys. 1994; 101:6141–6156.

[22]. Bauer BA, Warren GL, Patel S. Incorporating phase-dependent polarizability in nonadditive electrostatic models for molecular dynamics simulations of the aqueous liquid-vapor interface. J. Chem. Theory Comput. 2009; 5:359–373.

[23]. Lamoureux G, Roux B. Absolute hydration free energy scale for alkali and halide ions established from simulations with a polarizable force field. J. Phys. Chem. B. 2006; 110:3308–3322. [PubMed: 16494345]

[24]. Warren GL, Patel S. Hydration free energies of monovalent ions in transferable intermolecular potential four point fluctuating charge water: An assessment of simulation methodology and force field performance and transferability. J. Chem. Phys. 2007; 127:064509. [PubMed: 17705614]

[25]. Kumar S, Bouzida D, Swendsen RH, Kollman PA, Rosenberg JM. The weighted histogram analysis method for free-energy calculations on biomolecules. I. The method. J. Comp. Chem. 1992; 13:1011–1021.

[26]. Rose D, Benjamin I. Free energy of transfer of hydrated ion clusters from water to an immiscible organic solvent. J. Phys. Chem. B. 2009; 113:9296–9303. [PubMed: 19534541]

[27]. Carignano MA, Karlstrom G, Linse P. Polarizable ions in polarizable water: A molecular dynamics study. J. Phys. Chem. B. 1997; 101:1142–1147.

[28]. Rangei S, Klein ML. An ab initio study of water molecules in the bromide ion solvation shell. J. Chem. Phys. 2002; 116:196–202.

[29]. Rogers DM, Beck TL. Quasichemical and structural analysis of polarizable anion hydration. J. Chem. Phys. 2010; 132:014505. [PubMed: 20078170]

[30]. Brooks BR, Brooks CL III, MacKerell AD Jr. Nilsson L, Petrella RJ, Roux B, Won Y, Archontis G, Bartels C, Boresch S, Caflisch A, Caves L, Cui Q, Dinner AR, Feig M, Fisher S, Gao J, Hodoscek M, IM W, Kuczera K, Lazaridis T, Ma J, Ovchinnikov V, Paci E, Pastor RW, Post CB, Pu JZ, Schaefer M, Tidor B, Venable RM, Woodcock HL, Wu X, Yang W, York DM, Karplus M. CHARMM: The biomolecular simulation program. J. Comp. Chem. 2009; 30:1545–1614. [PubMed: 19444816]

[31]. Nosé S. A molecular dynamics methods for simulations in the canonical ensemble. Mol. Phys. 1984; 52:255–268.

[32]. Darden T, York D, Pedersen L. Particle mesh ewald: An $N \cdot \log(N)$ method for ewald sums in large systems. J. Chem. Phys. 1993; 98:10089–10092.

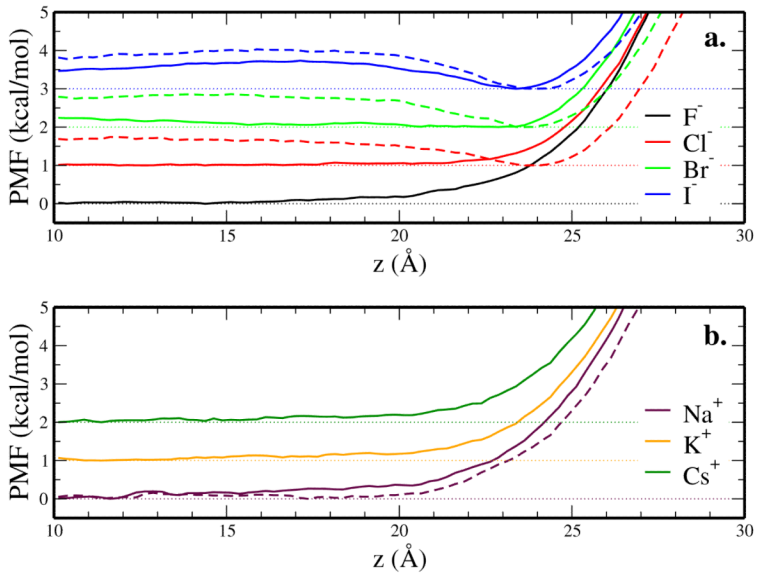

FIG. 1.

Potential of mean force for single ions across the TIP4P-FQ LV-interface. Solid lines represent ions in TIP4P-FQ, whereas dashed lines represent ions in TIP4P-QDP. A vertical offset of 1 kcal/mol is used to distinguish different anions/cations, with a dotted horizontal line denoting the minimum energy for each ion.

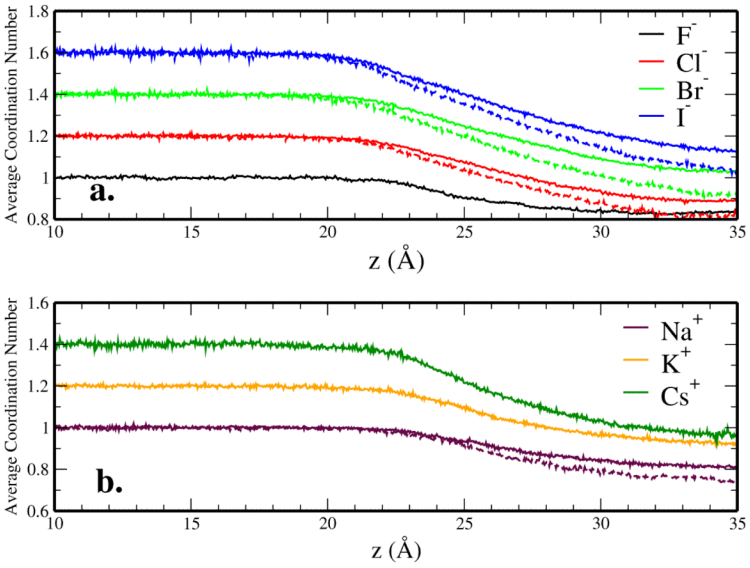

FIG. 2.

Variation of the number of water molecules coordinating (a) anions and (b) cations as a function of *z*-position expressed relative to the value in bulk. Solid lines represent ions in TIP4P-FQ, whereas dashed lines represent ions in TIP4P-QDP. Vertical offsets of 0.2 are imposed for visual clarity.

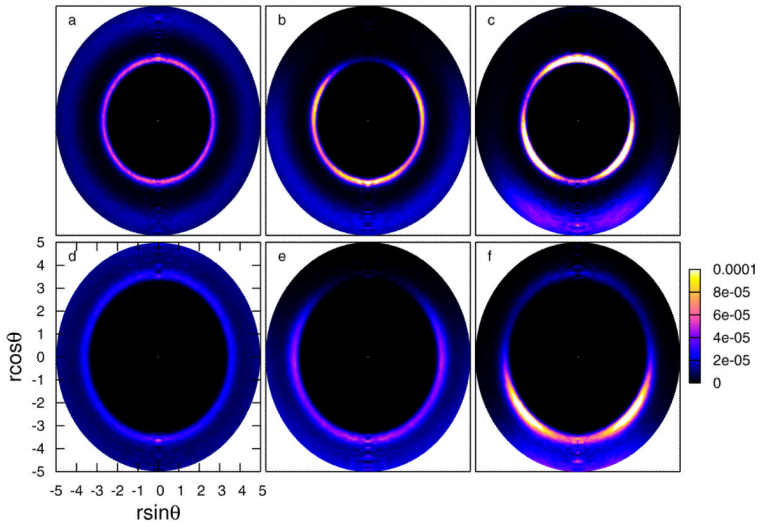

FIG. 3.

Radial Angular Distribution Functions for anions in TIP4P-FQ. Panel a-c represent F^- at z=10.0, 25.0 and 35.0 Å, respectively. Panel d-f show analogous plots for I^-

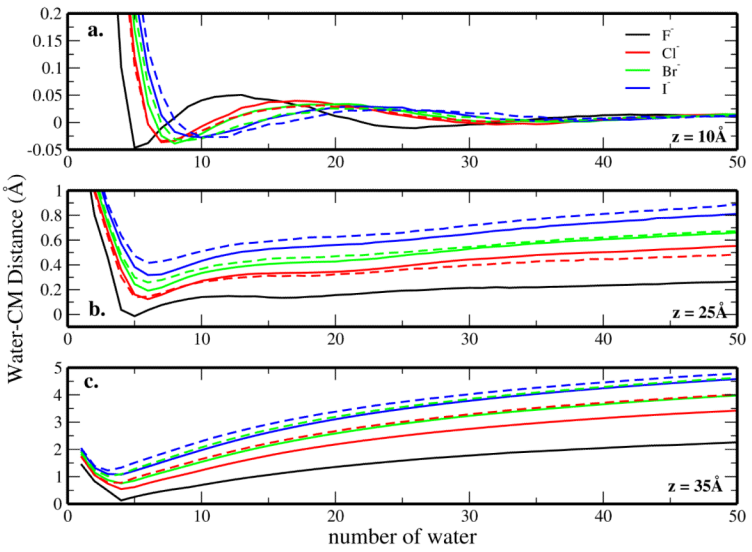

FIG. 4.

Analysis of anisotropy in anion solvation for ions in bulk water, at the LV-interface, and in vapor for TIP4P-FQ (solid lines) and TIP4P-QDP (dashed lines).

TABLE I

Hydration properties of ions in TIP4P-FQ and TIP4P-QDP

TIP4P-FQ	**ΔG_{hyd} (kcal/mol)[a,b]**	**R_{min} (Å)[b]**	**CN^{c}_{bulk}**	**CN_{gas}**	**ΔCN**
F^-	−112.83(9)	3.30	4.80 (4.83)	4.00	−0.80
Cl^-	−78.93(8)	3.79	6.25 (6.18)	4.31	−1.94
Br^-	−71.87(14)	3.93	6.60 (6.65)	4.18	−2.42
I^-	−63.15(15)	4.20	7.43 (7.46)	3.98	−3.45
Na^+	−98.41(12)	3.19	5.87 (5.88)	4.78	−1.09
K^+	−82.05(10)	3.62	7.11 (7.11)	5.17	−1.94
Cs^+	−69.63(8)	4.02	9.11 (9.11)	5.19	−3.92
TIP4P-QDP	ΔG_{hyd} (kcal/mol)[d]	R_{min} (Å)[e]	CN_{bulk}	CN_{gas}	ΔCN
Cl^-	−74.4(2)	3.80	6.00	3.70	−2.30
Br^-	−63.1(7)	4.10	6.89	3.57	−3.32
I^-	−57.5(1)	4.35	7.90	3.48	−4.42
Na^+	−103.2(1)	3.25	5.86	4.36	−1.50

[a] Hydration free energy from thermodynamic integration and appropriate correction terms including surface potential. Uncertainty in the last digit denoted in parentheses.

[b] Value from Ref.24

[c] Values in parentheses calculated via integration of the radial distribution function to the first minimum from Ref.24.

[d] Hydration free energies from thermodynamic integration and appropriate correction terms including surface potential.[20] Uncertainty in the last digit denoted in parentheses.

[e] Estimated from radial distribution functions of 1M NaX solutions.[20] Value for Na^+ determined from 1M NaCl RDF.